Portugaliae Electrochimica Acta 2019, 37(6), 335-344

DOI: 10.4152/pea.201906335

PORTUGALIAE ELECTROCHIMICA ACTA
ISSN 1647-1571

Inhibition of Aluminum Corrosion in 0.1 M Na_2CO_3 by Mentha pulegium

Hamdou Imane,[*] Essahli Mohamed and Lamiri Abdeslam

Univ. Hassan 1, Laboratory of Applied Chemistry and Environment, Faculty of Science and Technology, Settat-Morocco

Received February 3, 2017; accepted October 8, 2018

Abstract

The corrosion inhibition of aluminum, in 0.1 M Na_2CO_3, by *Mentha pulegium* essential oil, was studied using both polarization and impedance methods. The results show that *Mentha pulegium* is an effective inhibitor, providing an inhibition rate of 94.16 %, with a concentration of 800 ppm. The polarization study shows that the *Mentha pulegium* essential oil acted as a mixed inhibitor in 0.1 M Na_2CO_3. The activation energy calculation has proved that the inhibitor molecules adsorbed onto the aluminum surface, according to the physisorption mechanism.

Keywords: Aluminum, corrosion, inhibition, sodium carbonate, *mentha pulegium*.

Introduction

Aluminum is the second metal most used after iron, on an industrial scale [1-2], considering diversified advantages, such as low cost, light weight and good thermal and electrical conductivity [3]. The formation of the passivation layer onto the aluminum surface is the sole reason of its anti-corrosive immunity [2-6]; the latter is very soluble in aggressive media, with high concentrations of acids and bases [3-6]. The study of the aluminum behavior in aggressive media is required by virtue of these various industrial uses [4]. Several dangerous solutions have been adopted for aluminum protection, such as chromates, which are highly toxic and carcinogenic [4-10]. Therefore, the search for new green inhibitors to substitute chemical ones has become a requirement, because of their environmental friendliness and availability [11-15].

In this context, several works have been carried out on aluminum: Chaubey et al. [16] found that the papaya peel extract inhibits the aluminum corrosion in 1 M HCl, with an effectiveness of 95.5%. Nathiya et al. [17] compared the inhibitory efficacy of two extracts of *Dryopteris cochleata* leaves in 1 M H_2SO_4. The inhibitors were obtained by two different solvents (water and methanol). The results show that the methanol extract was more efficient (95.09%) than the aqueous extract (71.56%). Singh et al. [18] found that the *Piper longum* extract

[*] Corresponding author. E-mail address: imane.hamdou91@gmail.com

inhibits the aluminum corrosion in NaOH, with an efficiency of 89%. Abiola et al. [19] tested extracts of grains and leaves of *Gossypium hirsutum* on aluminum, in NaOH; both gave efficiencies that exceeded 90%. Abiola et al. [20] researched *Cocos nucifera* water to inhibit aluminum corrosion in HCl. Halambek et al. [21] evaluated the inhibitory power of *Laurus nobilis* oil in 3% NaCl, assuring an efficiency of 91.3%. Krishnaveni et al. [22] tested the aqueous extract of the leaves of *Morinda tinctoria* on aluminum in HCl, obtaining an efficiency of 96.72%, with a 2-hour immersion. Obi-Egbedi et al. [23] used the gravimetry technique to study the influence of the *Spondias mombin* extract on aluminum dissolution in H_2SO_4; the results show that this extract can protect aluminum against corrosion. Prabhu et al. [24] studied the effect of adding *Coriandrum sativum* grains extract to a phosphoric acid solution on the corrosion rate of aluminum; the obtained results ensure that this extract can be used as a green inhibitor.

The objective of our work was to join the topic of synthetic inhibitors substitution by the use of *Mentha pulegium* essential oil as an inhibitor of aluminum corrosion, in Na_2CO_3.

Experimental conditions

Steam distillation

The *Mentha pulegium* essential oil was obtained by steam distillation for 3 hours, using a Clevenger apparatus consisting of a balloon, balloon heater, refrigerant and a glass collector, where the distillation extracts were collected [25]. One part of this oil was used for the analysis of the chemical composition, while the other was dedicated for the anticorrosive tests. The chromatogram which illustrates the chemical composition of this oil is given in Fig. 1.

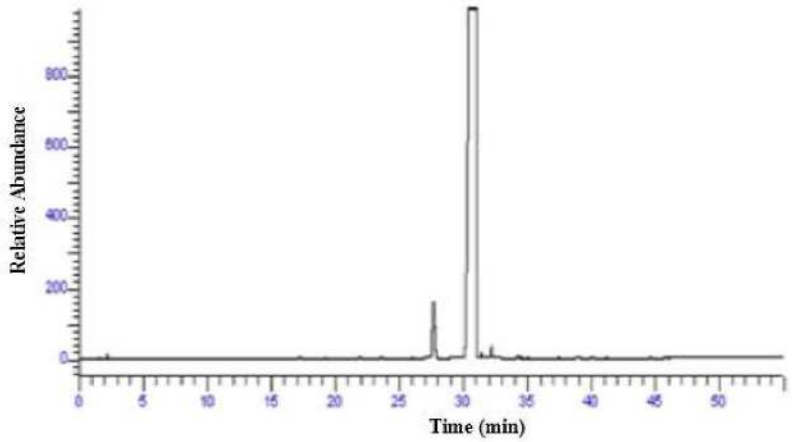

Figure 1. Chromatogram *of Mentha pulegium* essential oil.

Polarization and impedance

The electrochemical tests were performed in a three electrode cell: the working electrode was an aluminum disc with a surface of 1 cm^2; and platinum and saturated calomel electrodes were respectively used as auxiliary and reference electrodes. These electrodes were connected to a PGZ100

potentiostat/galvanostat linked to a computer controlled by "Volta master 4" software.
The polarization curves were obtained by varying, in a controlled manner, the potential applied to the working electrode between 1600 mV and -1200 mV, with a scanning rate of 0.5 mV / sec. The study of the temperature effect on the polarization and impedance was carried out in a temperature range from 288 K to 318 K, in the absence and presence of different inhibitor concentrations. The effectiveness of corrosion inhibition by the polarization method is calculated by equation (1), where I'_{cor} and I_{cor} respectively represent the current density with and without inhibitor.

$$E(\%) = \frac{I_{cor} - I'_{cor}}{I_{cor}} \times 100 \qquad (1)$$

Electrochemical impedance spectroscopy (EIS) measurements were performed with the same electrochemical system by imposing a sinusoidal perturbation and recording the response. Frequencies between 100 KHz and 10 Hz were superimposed on the corrosion potential.
The Nyquist curves represent the opposite of the imaginary component as a function of the real component; these diagrams give an idea of the phenomenon that took place at the electrode / solution interface. The impedance inhibition efficiency is calculated by equation 2, where R_T and R'_T respectively are the charge transfer resistance of aluminum in 0.1 M Na_2CO_3, with and without the presence of the inhibitor.

$$E(\%) = \frac{R_T - R'_T}{R_T} \times 100 \qquad (2)$$

Preparation of the solution

The corrosive medium was a 0.1 M solution of sodium bicarbonate prepared by dissolution in distilled water. The test solutions were prepared before each experiment by adding the extract to be directly tested into the electrochemical cell.

Table 1. Constituents of *Mentha pulegium* essential oil.

№	Retention time	Percentage (%)	Compound name
1	27.629	0.21	*Menthone*
2	30.403	14.72	*Geraniol*
3	30.426	84.75	*Pulegone*
4	31.146	0.02	*Isopulegyl acetate*
5	31.374	0.13	*Nopol*
6	32.181	0.03	*Cinnamyl alcohol «trans-»*
7	34.262	0.05	*Oocimenone E*
8	40.038	0.05	*Myristicin*

Results and discussion

Analysis of Mentha pulegium essential oil

The analysis of the chemical composition of *Mentha pulegium* essential oil allows determining 99% of its constituents (Table 1).

The major constituent of this oil is *Pulegone* (Fig. 2), with a percentage of 84.75%.

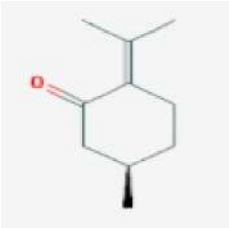

Figure 2. Chemical structure of Pulegone.

Effect of concentration

Polarization

The polarization curves of aluminum in 0.1 M Na_2CO_3, with and without inhibitor, are given in Fig. 3.

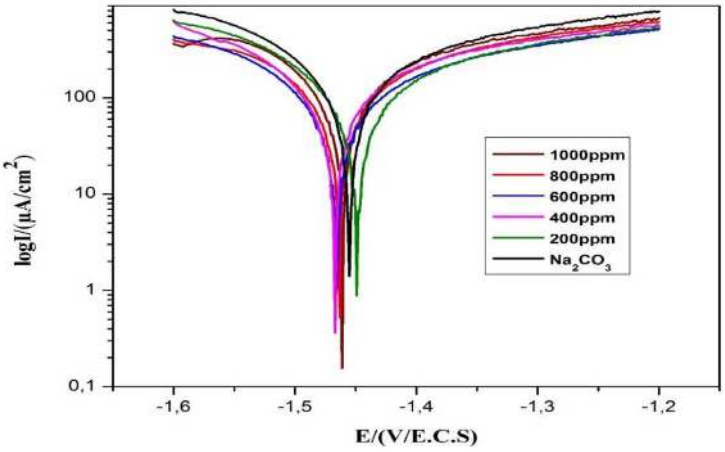

Figure 3. Polarization curves of aluminum in 0.1 M Na_2CO_3, with and without inhibitor, at 25 ± 0.1 °C.

Table 2 lists the electrochemical parameters (corrosion potential, E_{cor}, corrosion current, I_{cor}, inhibition efficiency, E, anodic Tafel slope, βa, and cathodic Tafel slope, βc).

Table 2. Electrochemical parameters of aluminum in 0.1 M Na_2CO_3, with and without the addition of *Mentha pulegium* essential oil at different concentrations.

C_{inh} (ppm)	E_{cor} (mV/ECS)	I_{cor} (µA/cm²)	β_a (mV)	β_c (mV)	E (%)
Blank	-1462.6	178.21	353.8	-248.6	----
200	-1451.1	25.67	48.1	-42.5	85.59
400	-1465.1	17.52	29.5	-30.3	90.16
600	-1468	14.62	24.9	-25.7	91.79
800	-1466.9	10.39	22.7	-20.9	94.16
1000	-1456.8	9.42	13	-12.6	94.71

The decrease in the two Tafel slopes with the increase in the extract concentration shows that *Mentha pulegium* essential oil is a mixed inhibitor, acting on both anodic and cathodic reactions by the formation of a protective film onto the aluminum surface [26-27]. The sharp decrease of the corrosion current density from 178.21 µA / cm^2 to 10.39 µA / cm^2 reflects that *Mentha pulegium* essential oil is a good inhibitor, reaching a maximum inhibition of 94.16%, at a concentration of 800 ppm.

Electrochemical impedance spectroscopy

Fig. 4 shows the Nyquist diagrams of aluminum in 0.1 M Na_2CO_3, without and with the addition of the inhibitor at different concentrations. The electrochemical parameters of these diagrams are given in Table 3.

The semicircular shape of the loops in the Nyquist diagram (Fig. 4) indicates that the aluminum corrosion in 0.1 M Na_2CO_3 was controlled by a charge transfer phenomenon [28]. The diameter of the loops raised with increasing concentrations, reflecting an enhancement in the charge transfer resistance and, thereafter, an increase in the inhibitor efficiency [29].

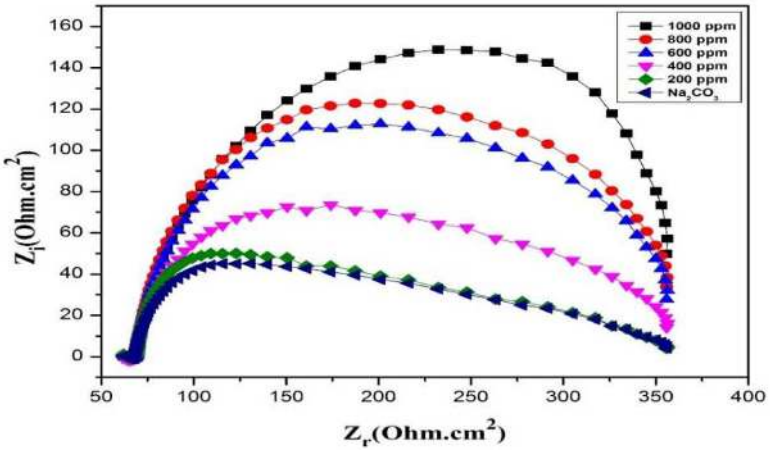

Figure 4. Nyquist curves of aluminum in 0.1 M Na_2CO_3, at different concentrations of *Mentha pulegium* essential oil, at 25 ± 0.1 °C.

The results in Table 3 show that the addition of the inhibitor led to an increase in R_T values, which measure the electron transfer across the surface [30-31] and hence, the rise of inhibition efficiency. The decrease in C_{dl} can be explained by the adsorption of the inhibitor molecules onto the aluminum surface, by forming an electronic double layer [32].

Table 3. Electrochemical parameters of aluminum in 0.1 M Na_2CO_3, with and without addition of the inhibitor.

C_{inh} (ppm)	R_T (ohm.cm^2)	C_{dl} (µF/cm^2)	E (%)
Blank	46.51	21.62	----
200	165.1	17.6	71.82
400	171.7	15.46	72.91
600	257.2	14.66	81.91
800	267.9	14.25	82.63
1000	271.3	13.3	82.85

In the equivalent electrical circuit given in Fig. 5, R_e is the resistance of the electrolyte, R_T is the charge transfer resistor and C_{dl} is the double layer capacitance.

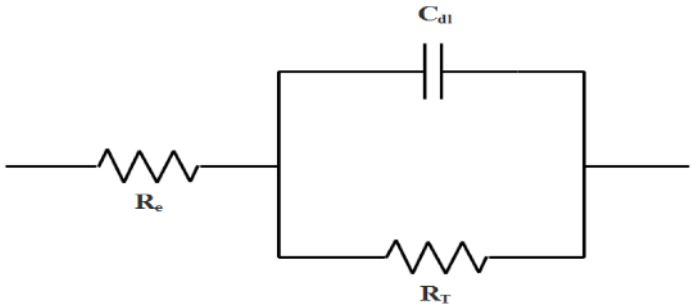

Figure 5. Equivalent circuit model for electrochemical impedance measurements.

Effect of temperature

Polarization

The polarization curves, with and without inhibitor, at different temperatures, are given in Figs. 6 and 7. The temperature influence on the electrochemical parameters is shown in Table 4. The increase in temperature makes the medium increasingly more corrosive, which results in an increase in the corrosion rate. The decrease in inhibitory efficiency (Table 4) can be explained by the hydrogen clearance on the metal surface, which causes desorption of the protective film [28].

Table 4. Electrochemical parameters of aluminum in 0.1 M Na_2CO_3 solution, with and without inhibitor, at different temperatures.

C_{inh} (ppm)	T (K)	I_{cor} ($\mu A/cm^2$)	E_{cor} (mV/ECS)	E (%)
Blank	288	103.32	-1439	----
	298	178.21	-1462.6	----
	308	197.93	-1509.4	----
	318	258.03	-1536.6	----
800 ppm	288	5.24	-1465	94.92
	298	10.39	-1466.9	94.16
	308	51.73	-1469.1	73.86
	318	110.67	-1501	57.10

Electrochemical impedance spectroscopy

The impedance curves obtained at different temperatures, with and without inhibitor, are presented in Figs. 8 and 9. The electrochemical parameters are grouped in Table 5.

The increase in temperature led to a sharp decrease in R_T and, consequently, to a reduction of the inhibition efficiency (Table 5). This was due to the fixation of the inhibitor molecules onto the aluminum surface, according to a physical adsorption mechanism [33].

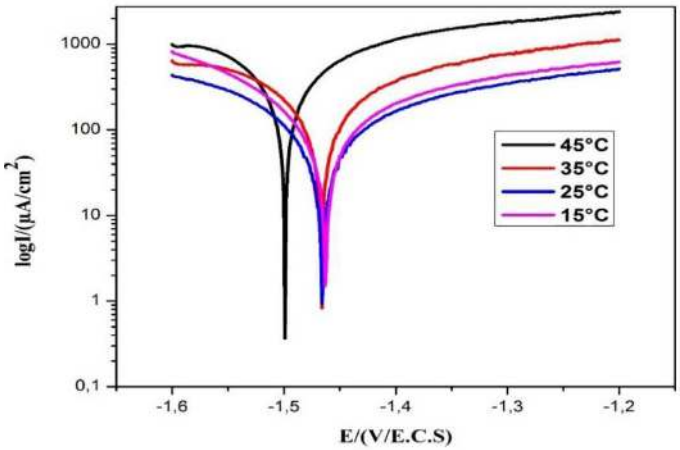

Figure 6. Polarization curves of aluminum in 0.1 M Na_2CO_3, without inhibitor, at different temperatures.

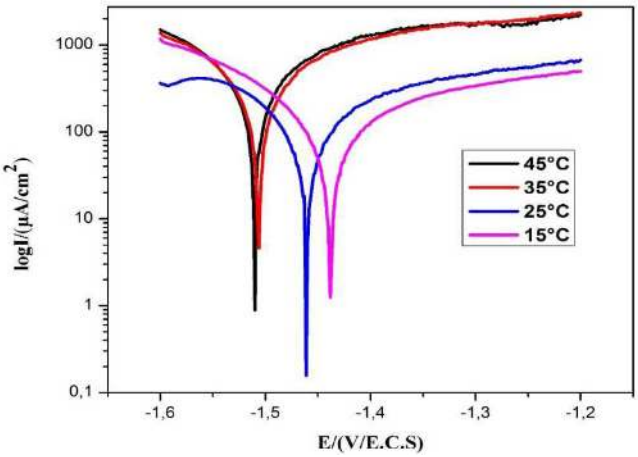

Figure 7. Polarization curves of aluminum in 0.1 M Na_2CO_3, with the presence of 800 ppm of the inhibitor, at different temperatures.

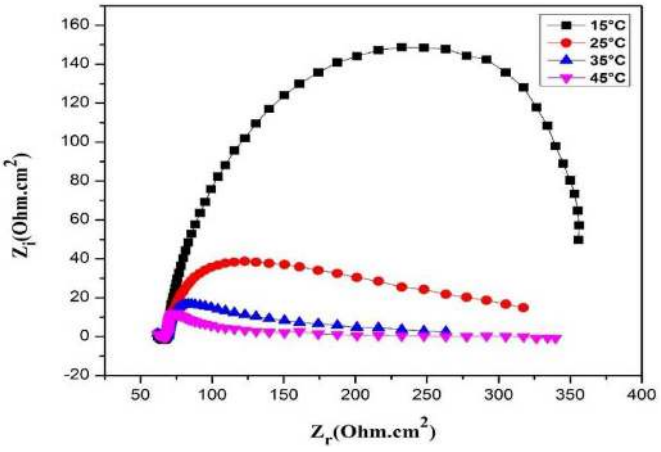

Figure 8. Nyquist curves of aluminum in 0.1 M Na_2CO_3, without inhibitor, at different temperatures.

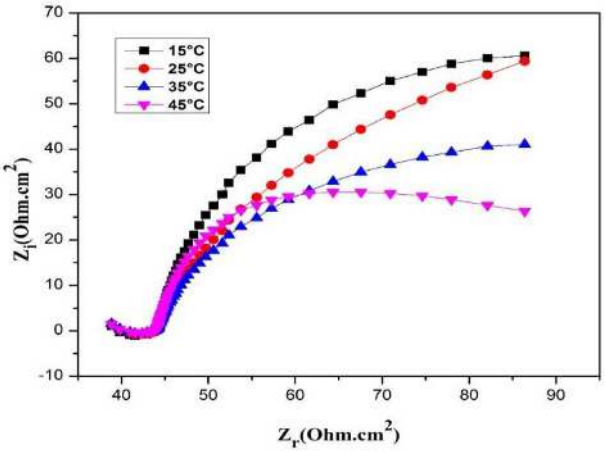

Figure 9. Nyquist curves of aluminum in 0.1 M Na_2CO_3, with 800 ppm of the inhibitor, at different temperatures.

Table 5. Electrochemical parameters of aluminum impedance diagram, with and without inhibitor, at different temperatures.

C_{inh} (ppm)	T (K)	R_T (ohm.cm^2)	E (%)
Blank	288	55.67	----
	298	46.51	----
	308	39.72	----
	318	22.3	----
800 ppm	288	358.5	84.47
	298	267.9	82.63
	308	138.9	71.40
	318	72.31	69.16

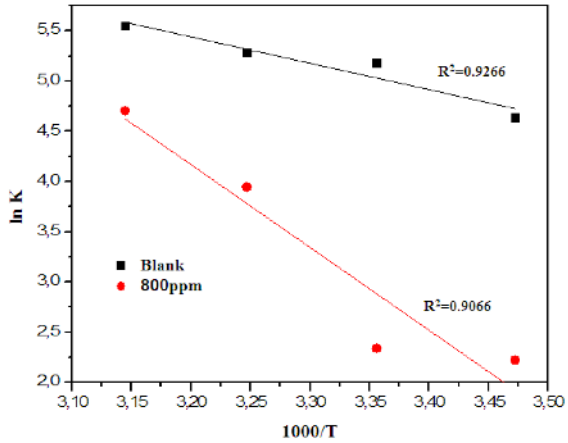

Figure 10. Arrhenius curves of aluminum in 0.1 M Na_2CO_3, with and without inhibitor.

Determination of activation energy

The Arrhenius equation (3), where K is the corrosion rate, A is the Arrhenius factor and E_a is the activation energy, was used to study the inhibition mechanism of aluminum corrosion. The Arrhenius diagrams of aluminum dissolution in 0.1 M Na_2CO_3, with and without inhibitor, are shown in Fig. 10.

$$K = Ae^{-E_a/RT} \qquad (3)$$

The calculated values of the activation energy, with and without inhibitor, are, respectively, 68.57 KJ/mol and 21.82 KJ/mol. The activation energy increase in the presence of the essential oil of *Mentha pulegium* indicates that the inhibition was achieved by a mechanism of physisorption [34-35].

Conclusions

- The major constituent of *Mentha pulegium* essential oil is *Pulegone*, within a percentage of 84.75%.
- The essential oil of *Mentha pulegium* provides an inhibition efficiency of 94.16%, with a concentration of 800 ppm.
- The slowing down of the corrosion rate was manifested by the reduction of the anodic and cathodic Tafel slopes; with the progressive addition of the extract, the *Mentha pulegium* essential oil acted as a mixed inhibitor.
- The corrosion inhibition occurred by adsorption of the inhibitor molecules onto the aluminum surface, by forming weak bonds.

References

1. Prabhu D, Rao PJ. Environ Chem Eng. 2013;1:676.
2. Verma C, Singh P, Bahadur I, et al. J Mol Liq. 2015;209:767.
3. Awad MK, Metwally MS, Soliman SA, et al. J Ind Eng Chrom. 2014;20:796.
4. Oguzie EE. Corros Sci. 2007;49:1527.
5. El-Etre AY. Corros Sci. 2003;45:2485.
6. Li X, Deng S, Fu H. Corros Sci. 2011;53:2748.
7. Kartsonakis IA, Balaskas AC, Kordas GC. Corros Sci. 2011;53:3771.
8. Emregül KC, Aksüt AA. Corros Sci. 2003;45:2415.
9. Khaled KF. Corros Sci. 2010;52:2905.
10. Kwolek P, Kamiński A, Dychtoń K. Corros Sci. 2016;106:208.
11. El-Etre AY, Abdallah M, El-Tantawy ZE. Corros Sci. 2005;47:385.
12. Deng S, Li X. Corros Sci. 2012;55:407.
13. Mourya P, Banerjee S, Singh MM. Corros Sci. 2014;85:352.
14. Ji G, Anjum S, Sundaram S. Corros Sci. 2015;90:107.
15. Fuchs-Godec R, Zerjav G. Corros Sci. 2015;97:7.
16. Chaubey N, Kumar V, Quraishi MA. Ain Shams Eng J. 2016.
17. Nathiya RS, Raj V. Egypt J Pet. 2016.
18. Singh A, Ahamad I, Quraishi MA. Arab J Chem. 2012.
19. Abiola OK, Otaigbe JOE, Kio OJ. Corros Sci. 2009;51:1879.
20. Abiola OK, Tobun Y. Chinese Chem Lett. 2010;21:1449.
21. Halambek J, Berkovi K, Vorkapi J. Mater Chem Phys J. 2013;137:788.
22. Krishnaveni K, Ravichandran J. Trans Nonferrous Met Soc China. 2014;24:2704.
23. Obi-Egbedi NO, Obot IB, Umoren SA. Arab J Chem. 2012;3:361.

24. Prabhu D, Rao P. J Environ Chem Eng. 2013.
25. Fadil M, Farah A, Ihssane B, et al. J Mater Environ Sci. 2015;6:2346.
26. Houbairi S, Lamiri A, Essahli M. Int J Eng Res Tech. 2014;3:698.
27. Abdallah M, Kamar EM, Eid S, et al. J Mol Liq. 2016;220:755.
28. Vengatesh G, Karthik G, Sundaravadivelu M. Egypt J Pet. 2016.
29. Liao LL, Mo S, Lei JL, et al. J Colloid Interface Sci. 2016;474:68.
30. Bensabah F, Essahli M, Lamiri A, et al. Port Electrochim Acta. 2014;32:381-393.
31. Badiea AM, Mohana KN. J Mater Eng Perform. 2009;18:1264.
32. Houbairi S, Lamiri A , Essahli M. Chem Sci Rev Lett. 2014;3:353.
33. Azzouyahar E, Bazzi L, Belkhaouda M. RS Publication Com. 2014;4:941.
34. Geetha S, Lakshmi S, Bharathi K. Int J Adv Sci Tech Res. 2013;3:258.
35. Zarrouk A, Al-Deyab SS. Int J Electrochem Sci. 2011;6:6261.